

See discussions, stats, and author profiles for this publication at: <https://www.researchgate.net/publication/5328849>

# Ambient Aerodynamic Ionization Source for Remote Analyte Sampling and Mass Spectrometric Analysis

ARTICLE *in* ANALYTICAL CHEMISTRY · AUGUST 2008

Impact Factor: 5.64 · DOI: 10.1021/ac800289f · Source: PubMed

---

CITATIONS

20

---

READS

38

## 4 AUTHORS, INCLUDING:



[Adam M Hawkrige](#)

Virginia Commonwealth University

48 PUBLICATIONS 1,649 CITATIONS

SEE PROFILE



[David Muddiman](#)

North Carolina State University

256 PUBLICATIONS 6,919 CITATIONS

SEE PROFILE

# Ambient Aerodynamic Ionization Source for Remote Analyte Sampling and Mass Spectrometric Analysis

R. Brent Dixon, Jason S. Sampson, Adam M. Hawkridge,\* and David C. Muddiman\*

W. M. Keck FT-ICR Mass Spectrometry Laboratory, Department of Chemistry, North Carolina State University, Raleigh, North Carolina 27695

The use of aerodynamic devices in ambient ionization source development has become increasingly prevalent in the field of mass spectrometry. In this study, an air ejector has been constructed from inexpensive, commercially available components to incorporate an electrospray ionization emitter within the exhaust jet of the device. This novel aerodynamic device, herein termed remote analyte sampling, transport, and ionization relay (RASTIR) was used to remotely sample neutral species in the ambient and entrain them into an electrospray plume where they were subsequently ionized and detected using a linear ion trap Fourier transform mass spectrometer. Two sets of experiments were performed in the ambient environment to demonstrate the device's utility. The first involved the remote (~1 ft) vacuum collection of pure sample particulates (i.e., dry powder) from a glass slide, entrainment and ionization at the ESI emitter, and mass spectrometric detection. The second experiment involved the capture (vacuum collection) of matrix-assisted laser desorbed proteins followed by entrainment in the ESI emitter plume, multiple charging, and mass spectrometric detection. This approach is in principle a RASTIR-assisted matrix-assisted laser desorption electrospray ionization source (Sampson, J. S.; Hawkridge, A. M.; Muddiman, D. C. *J. Am. Soc. Mass Spectrom.* 2006, 17, 1712–1716; *Rapid Commun. Mass Spectrom.* 2007, 21, 1150–1154.). A detailed description of the device construction, operational parameters, and preliminary small molecule and protein data are presented.

Aerodynamic and hydrodynamic injectors/ejectors have been utilized in a multitude of applications starting with steam engines in the later half of the 19th century. Additional examples include vacuum and exhaust pumps, reactors in industrial applications (e.g., transport phenomena), and water aspirators.<sup>4–9</sup> Although the functional characteristics and applications of these devices

vary, the operational principles are largely dependent on the Venturi effect. The Venturi effect is based on Bernoulli's principle (i.e., conservation of energy), where a reduced-pressure region (i.e., vacuum) is created from the conversion of a high-pressure fluid (gas or liquid) to a high-velocity jet.<sup>10</sup> The potential utility of these devices toward ambient ionization source development in mass spectrometry was recently demonstrated by Zhou et al.,<sup>11</sup> where an air amplifier was used to improve ion transmission in the electrospray process thereby lowering detection limits. Subsequent studies using this device,<sup>12–15</sup> the introduction of a commercial air ejector for remote ion transport and mass spectrometric detection,<sup>16</sup> and the continued expansion of novel ambient ionization sources<sup>1,2,17–41</sup> have created a wealth of opportunities in the field of mass spectrometry.

\* To whom correspondence should be addressed. E-mail: adam\_hawkridge@ncsu.edu. Phone: 919-513-7947. Fax: 919-513-7993. E-mail: david\_muddiman@ncsu.edu. Phone: 919-513-0084. Fax: 919-513-7993.

- (1) Sampson, J. S.; Hawkridge, A. M.; Muddiman, D. C. *J. Am. Soc. Mass Spectrom.* 2006, 17, 1712–1716.
- (2) Sampson, J. S.; Hawkridge, A. M.; Muddiman, D. C. *Rapid Commun. Mass Spectrom.* 2007, 21, 1150–1154.
- (3) Kneass, S. L. *Practice and Theory of the Injector*, 3rd ed.; John Wiley & Sons: New York, 1910.

- (4) Keenan, J. H.; Neumann, E. P.; Lustwerk, F. J. *Appl. Mech.* 1950, 17, 299–309.
- (5) Davies, G. S.; Mitra, A. K.; Roy, A. N. *Ind. Eng. Chem. Process Des. Dev.* 1967, 6, 293–299.
- (6) Matsuo, K.; Sasaguchi, K.; Tasaki, K.; Mochizuki, H. *Bull. JSME, Jpn. Soc. Mech. Eng.* 1981, 24, 2090–2097.
- (7) Matsuo, K.; Sasaguchi, K.; Kiyotoki, Y.; Mochizuki, H. *Bull. JSME, Jpn. Soc. Mech. Eng.* 1982, 25, 1898–1905.
- (8) Matsuo, K.; Mochizuki, H.; Kobayashi, A. *Bull. JSME, Jpn. Soc. Mech. Eng.* 1986, 29, 1434–1439.
- (9) Matsuo, K.; Mochizuki, H.; Nakamura, T. *Bull. JSME, Jpn. Soc. Mech. Eng.* 1986, 29, 3297–3302.
- (10) Jackson, M. L. *AIChE J.* 1964, 10, 836–842.
- (11) Zhou, L.; Yue, B. F.; Dearden, D. V.; Lee, E. D.; Rockwood, A. L.; Lee, M. L. *Anal. Chem.* 2003, 75, 5978–5983.
- (12) Hawkridge, A. M.; Zhou, L.; Lee, M. L.; Muddiman, D. C. *Anal. Chem.* 2004, 76, 4118–4122.
- (13) Yang, P. X.; Cooks, R. G.; Ouyang, Z.; Hawkridge, A. M.; Muddiman, D. C. *Anal. Chem.* 2005, 77, 6174–6183.
- (14) Dixon, R. B.; Muddiman, D. C. *Rapid Commun. Mass Spectrom.* 2007, 21, 3207–3212.
- (15) Dixon, R. B.; Muddiman, D. C.; Hawkridge, A. M.; Fedorov, A. G. *J. Am. Soc. Mass Spectrom.* 2007, 18, 1909–1913.
- (16) Dixon, R. B.; Bereman, M. S.; Hawkridge, A. M.; Muddiman, D. C. *J. Am. Soc. Mass Spectrom.* 2007, 18, 1844–1847.
- (17) Kolaitis, L.; Lubman, D. M. *Anal. Chem.* 1986, 58, 2137–2142.
- (18) Coon, J. J.; McHale, K. J.; Harrison, W. W. *Rapid Commun. Mass Spectrom.* 2002, 16, 681–685.
- (19) Chang, D. Y.; Lee, C. C.; Shiea, J. *Anal. Chem.* 2002, 74, 2465–2469.
- (20) Shieh, I. F.; Lee, C. Y.; Shiea, J. *J. Proteome Res.* 2005, 4, 606–612.
- (21) McEwen, C. N.; McKay, R. G.; Larsen, B. S. *Anal. Chem.* 2005, 77, 7826–7831.
- (22) McEwen, C.; Gutteridge, S. J. *Am. Soc. Mass Spectrom.* 2007, 18, 1274–1278.
- (23) Cody, R. B.; Laramée, J. A.; Durst, H. D. *Anal. Chem.* 2005, 77, 2297–2302.
- (24) Fernandez, F. M.; Cody, R. B.; Green, M. D.; Hampton, C. Y.; McGready, R.; Sengaloudeth, S.; White, N. J.; Newton, P. N. *Chem. Med. Chem.* 2006, 1, 702–705.

Several novel ambient ionization sources, herein described as hybrid ionization sources due to their modification of “traditional” ionization mechanisms (e.g., ESI, MALDI, APPI, APCI), have been recently introduced including laser desorption atmospheric pressure ionization,<sup>17,18</sup> fused droplet-electrospray ionization (FD-ESI),<sup>19,20</sup> atmospheric-pressure solids analysis probe (ASAP),<sup>21,22</sup> direct analysis in real time,<sup>23–25</sup> desorption electrospray ionization (DESI),<sup>26–32</sup> extractive electrospray ionization (EESI),<sup>33–37</sup> electrospray-assisted laser desorption/ionization,<sup>38–40</sup> matrix-assisted laser desorption electrospray ionization (MALDESI),<sup>1,2</sup> and laser ablation electrospray ionization.<sup>41</sup> Although these methods provide innovative ionization pathways, the proximity of sample to the mass spectrometer’s sampling orifice (within centimeters) can be a limiting constraint when considering large or remote sampling substrates, especially nonvolatile samples on solid substrates as recently demonstrated by Cooks et al. using a miniature mass spectrometer.<sup>42–44</sup> Furthermore, combining multiple ionization sources (e.g., MALDI+ESI in MALDESI) can be problematic where isolation of electrostatic voltages (e.g., target, ESI emitter, and MS inlet), analyte capture and transport efficiency, and localization of the analyte–ionization source can be less than optimal. The need for directed capture and transport (locally or remotely) of analytes followed by ionization for mass spectrometric detection provides the impetus for this research.

A recent report from this laboratory introduced the concept of using an air ejector to transport remotely generated ions to the entrance of the mass spectrometer.<sup>16</sup> The device had some notable advantages over alternative remote sampling methods<sup>45,46</sup> including flexible tubing, low cost, and amenability to other mass

spectrometer inlets (e.g., Micromass Z-spray). Furthermore, the operation and configuration of the air ejector has the potential for allowing post-transport ionization of neutrals using a multitude of sources such as ESI, APCI, and APPI. A series of recent reports have shown the potential of post-transport ionization via ESI using either FD-ESI<sup>19,20</sup> or EESI.<sup>33–37</sup> Both of these techniques are designed to entrain volatile or semivolatile neutral molecular species into an ESI plume to facilitate ionization and mass spectrometric detection. A limitation to both of these approaches is their inability to collect and subsequently ionize from a nonvolatile substrate (e.g., sample spotted on MALDI target) such as biological or synthetic macromolecules.

The remote analyte sampling, transport, and ionization relay (RASTIR) source described herein incorporates several aspects of the techniques described above including MALDESI, air amplifier/air ejection, FD-ESI, and EESI to provide a direct means of locally or remotely collecting nonvolatile neutral analytes for subsequent ionization in ESI. Two sets of experiments were performed to demonstrate the function and utility of the RASTIR device. The first involved the remote/vacuum collection, transport, and ESI ionization of neutral sample particulates (i.e., dry powder) from a glass slide. The second experiment involved the capture (vacuum collection) of matrix-assisted laser desorbed proteins B-type natriuretic peptide (BNP-32) and ubiquitin followed by entrainment in the ESI emitter plume, multiple charging, and mass spectrometric detection. The RASTIR device is relatively inexpensive (<\$100), easy to construct from commercially available components, and adaptable to other ionization techniques.

## EXPERIMENTAL SECTION

**Materials.** Acetaminophen, caffeine, b-type natriuretic peptide-32 (BNP-32), ubiquitin, 2,5 dihydroxybenzoic acid (DHB) and formic acid were obtained from Sigma Aldrich (St. Louis, MO) and used without further purification. HPLC grade acetonitrile and water were purchased from Burdick & Jackson (Muskegon, MI). Nitrogen (99.98%) and LTQ helium bath gas (99.999%) were obtained from MWSC High Purity Gases (Raleigh, NC).

**Methods.** The ESI solution was prepared by mixing 1:1 acetonitrile and water (v/v) with 0.1% formic acid. The matrix solution was prepared by dissolving 150 mg of DHB in 1 mL of 1:1 H<sub>2</sub>O/ACN with 0.1% formic acid. BNP-32 and ubiquitin were subsequently dissolved in this ESI solution at 288 and 500  $\mu$ M, respectively. These were then mixed 1:1 with DHB matrix for sample solutions of 144 and 250  $\mu$ M of BNP-32 and ubiquitin, respectively. Each MALDI spot was prepared by depositing 0.8  $\mu$ L of each sample solution onto the stainless steel MALDI target (P/N 4333375, Applied Biosystems, Foster City, CA) followed by active drying in the ambient<sup>47</sup> immediately prior to MALDESI-RASTIR analysis.

**Mass Spectrometry.** Mass spectra were acquired in the positive-ion mode on a LTQ-FT mass spectrometer (Thermo Fisher, San Jose, CA) equipped with an actively shielded 7-T superconducting magnet (Oxford Instruments, Concord, MA). The automatic gain control was turned off and the maximum ionization time set at 1 s for the MALDESI-RASTIR measurements. The maximum ionization time for the vacuum desorbed particulate

- (25) Petucci, C.; Diffendal, J.; Kaufman, D.; Mekonnen, B.; Terefenko, G.; Musselman, B. *Anal. Chem.* **2007**, *79*, 5064–5070.
- (26) Takats, Z.; Wiseman, J. M.; Gologan, B.; Cooks, R. G. *Science* **2004**, *306*, 471–473.
- (27) Takats, Z.; Wiseman, J. M.; Cooks, R. G. *J. Mass Spectrom.* **2005**, *40*, 1261–1275.
- (28) Bereman, M. S.; Nyadong, L.; Fernandez, F. M.; Muddiman, D. C. *Rapid Commun. Mass Spectrom.* **2006**, *20*, 3409–3411.
- (29) Venter, A.; Cooks, R. G. *Anal. Chem.* **2007**, *79*, 6398–6403.
- (30) Bereman, M. S.; Williams, T. I.; Muddiman, D. C. *Anal. Chem.* **2007**, *79*, 8812–8815.
- (31) Cooks, R. G.; Ouyang, Z.; Takats, Z.; Wiseman, J. M. *Science* **2006**, *311*, 1566–1570.
- (32) Venter, A.; Sojka, P. E.; Cooks, R. G. *Anal. Chem.* **2006**, *78*, 8549–8555.
- (33) Chen, H. W.; Venter, A.; Cooks, R. G. *Chem. Commun.* **2006**, 2042–2044.
- (34) Chen, H. W.; Sun, Y. P.; Wortmann, A.; Gu, H. W.; Zenobi, R. *Anal. Chem.* **2007**, *79*, 1447–1455.
- (35) Chen, H. W.; Wortmann, A.; Zenobi, R. *J. Mass Spectrom.* **2007**, *42*, 1123–1135.
- (36) Chen, H.; Yang, S.; Wortmann, A.; Zenobi, R. *Angew. Chem. Int. Ed.* **2007**, *46*, 7591–7594.
- (37) Chen, H. W.; Touboul, D.; Jecklin, M. C.; Zheng, J.; Luo, M. B.; Zenobi, R. N. *Eur. J. Mass Spectrom.* **2007**, *13*, 273–279.
- (38) Shiea, J.; Huang, M. Z.; Hsu, H. J.; Lee, C. Y.; Yuan, C. H.; Beech, I.; Sunner, J. *Rapid Commun. Mass Spectrom.* **2005**, *19*, 3701–3704.
- (39) Huang, M. Z.; Hsu, H. J.; Lee, L. Y.; Jeng, J. Y.; Shiea, L. T. *J. Proteome Res.* **2006**, *5*, 1107–1116.
- (40) Peng, I. X.; Shiea, J.; Loo, R. R. O.; Loo, J. A. *Rapid Commun. Mass Spectrom.* **2007**, *21*, 2541–2546.
- (41) Nemes, P.; Vertes, A. *Anal. Chem.* **2007**, *79*, 8098–8106.
- (42) Badman, E. R.; Cooks, R. G. *J. Mass Spectrom.* **2000**, *35*, 659–671.
- (43) Gao, L.; Song, Q. Y.; Patterson, G. E.; Cooks, R. G.; Ouyang, Z. *Anal. Chem.* **2006**, *78*, 5994–6002.
- (44) Chaudhary, A.; van Amerom, F. H. W.; Short, R. T.; Bhansali, S. *Int. J. Mass Spectrom.* **2006**, *251*, 32–39.
- (45) Cotte-Rodriguez, I.; Cooks, R. G. *Chem. Commun.* **2006**, 2968–2970.
- (46) Cotte-Rodriguez, I.; Mulligan, C. C.; Cooks, G. *Anal. Chem.* **2007**, *79*, 7069–7077.

- (47) Williams, T. I.; Saggese, D. A.; Wilcox, R. J.; Martin, J. D.; Muddiman, D. C. *Rapid Commun. Mass Spectrom.* **2007**, *21*, 807–811.

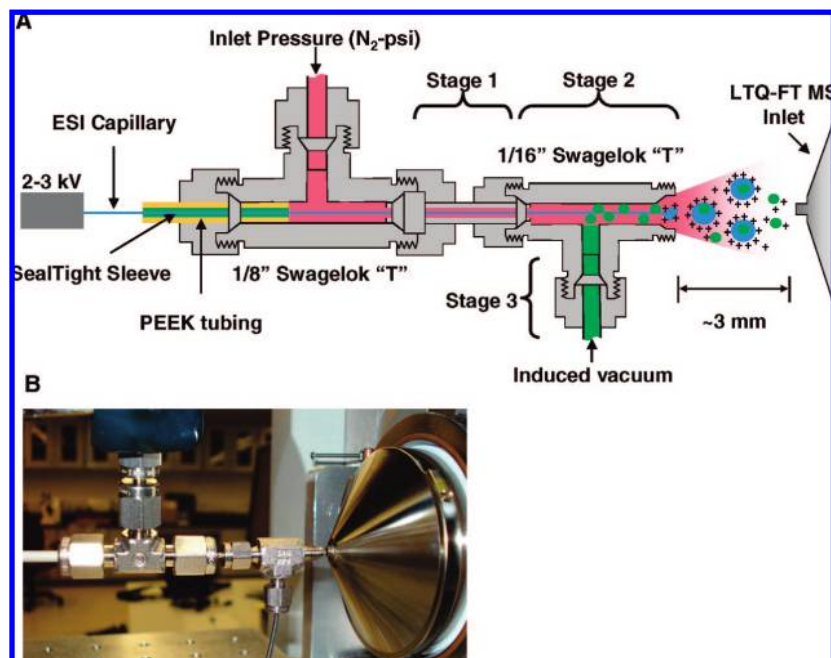


**Figure 1.** (A) Labeled schematic of the RASTIR assembly showing the high-pressure region (stage 1), high-velocity jet/entrainment/exhaust region (stage 2), and the vacuum region (stage 3). (B) Photograph of the RASTIR source interface to the front of an LTQ-FT MS.

measurements was 50 ms. The unmodified heated metal capillary temperature was maintained at 250 °C and 37 V.

**RASTIR Source.** The RASTIR source was constructed of several Swagelok fittings with minor modifications and readily available HPLC parts from Upchurch Scientific. See Supporting Information for a complete parts list. The prototype described herein was based on a nebulizer and air ejector design by Kotrappa et al.<sup>48</sup> Figure 1 shows the RASTIR assembly coupled to the inlet of the LTQ-FT MS. A single unmodified stainless steel 1/8-in. Swagelok Tee (P/N SS-200-3, Raleigh Valve and Fitting, Raleigh, NC) was coupled to a single modified (inner diameter of linear portion machined from 0.06 to 0.09 in.) stainless steel 1/16-in. Swagelok Tee (P/N SS-100-3, Raleigh Valve and Fitting) via a 750  $\mu\text{m}$  i.d.  $\times$  1/16 in. o.d. stainless steel tubing (P/N SS-201-PC-1, Raleigh Valve and Fitting). Pressurized nitrogen was metered into this assembly via a 1/4-in. polyethylene tubing (P/N 14176121, Thermo Fisher Scientific, Pittsburgh, PA) using a 1/4–1/8-in. Swagelok fitting (P/N SS-400-6-2, Raleigh Valve and Fitting) and a 1/8-in. port connector (P/N SS-201-pc, Raleigh Valve and Fitting). The assembly houses a length of fused-silica capillary (50  $\mu\text{m}$  i.d., 360  $\mu\text{m}$  o.d., P/N 2000017, Polymicro Technologies, Inc., Phoenix, AZ), which transports the ESI solvent at a flow rate of 1–10  $\mu\text{L}/\text{min}$ . The capillary is held in place by tightening the outer 1/8-in. Swagelok nut around a portion of PEEK tubing (1/8 in. o.d., 0.062 in. i.d., P/N 1534, Upchurch Scientific, Oak Harbor, WA), which is concentric around a silica SealTight FEP tubing sleeve (1/16 in. o.d., 0.015 in. i.d., P/N F-242x, Upchurch Scientific). A 10-in. length of flexible PEEK tubing (1/16 in. o.d., 0.04 in. i.d., P/N 1538 Upchurch Scientific) was used as the “vacuum collection tube” for the particulate experiments to allow rapid switching between analytes. PEEK (1/16 in. o.d., 0.04 in. i.d., P/N 1538 Upchurch Scientific) and stainless steel tubing (P/N T40C20, VICI Valco

Instruments Co. Inc., Houston, TX) were cut to  $\sim 3$  in. to sample the MALDESI-generated neutral analytes. The metal tubing allowed more consistent placement of the tubing over the sample spot during the laser desorption. The nebulizing gas pressures for both particulate and MALDESI experiments were measured at the high-pressure regulator (P/N 2053021-01-000, Controls Corp. of America, Virginia Beach, VA) ranging from 10 to 40 psi. At 20 psi applied pressure, a vacuum of 13 mmHg (measured with a Mannix Hand-held digital manometer P/N DM8200, Hauppauge, NY) is achieved at the terminus of the vacuum collection tube. A plot showing the full characteristics of the device can be found in Supporting Information. A 2–3.5 kV ESI voltage was applied at a stainless steel VALCO union  $\sim 6$ –8 in. from the emitter tip while the stainless steel RASTIR assembly was held at ground potential.

**MALDESI Source.** The MALDESI source used in these experiments implements an Explorer 349-nm laser (P/N Expl-349-120-1KE, Newport Corp., Irvine, CA), two UV enhanced directional mirrors (P/N 10D20AL.2, Newport Corp.), and a fused-silica focusing lens (P/N SPX017+AR.10, Newport Corp.). The laser was fired at a repetition rate of 20 Hz and laser power of 53  $\mu\text{J}$  (measured at the laser source). The laser beam was focused at  $\sim 45^\circ$  relative to the sample surface to create elliptical spot size of  $\sim 60 \mu\text{m} \times 80 \mu\text{m}$  diameter. The sample target was moved by the motor-driven XYZ stage (P/N 436, Newport Corp.) with a computer-controlled motion system (P/N ESP 300-11N1N1, Newport Corp.). The laser desorbed material was entrained by the induced vacuum at the terminus of the vacuum collection tube placed in close proximity ( $\sim 1$  mm) to the laser beam incidence spot on the sample. The material was transported through the RASTIR device to the electrospray ionization region where it was ionized by interactions with electrosprayed solvent droplets.

## RESULTS AND DISCUSSION

**RASTIR Interface.** Figure 1 shows the experimental configuration of the RASTIR source including a labeled schematic of

(48) Kotrappa, P.; Mayya, Y. S.; Raghunath, B.; Menon, V. B.; Bhandi, D. P. *Ann. Occup. Hyg.* **1976**, *19*, 363–366.



the device (Figure 1A). The emitter/exhaust of the RASTIR source was held in front of the LTQ-FT MS inlet at a distance of approximately 3 mm along the axis of the heated metal capillary (Figure 1B). The device is described in 3 stages; high pressure (stage 1), high velocity jet/entrainment/exhaust (stage 2), and vacuum collection tube (stage 3). One of the principle design components of the RASTIR device is that the cross-sectional area for fluid flow within stage 1 should be significantly smaller than stage 2 to achieve a high velocity secondary flow (i.e., entrainment and exhaust). Equation 1 defines the available cross-sectional area for fluid flow,  $\alpha_{\text{stage1}}$ , where  $\alpha_{\text{port}}$  and  $\alpha_{\text{capillary}}$  are the cross-sectional areas of the port connector (750  $\mu\text{m}$ ) and the fused silica capillary (360  $\mu\text{m}$ ) respectively.

$$\alpha_{\text{stage1}} = \alpha_{\text{port}} - \alpha_{\text{capillary}} \quad (1)$$

It is imperative that the cross-sectional area of stage 2,  $\alpha_{\text{stage2}}$  be much larger than stage 1 such that back pressure is minimized. Finally the cross-sectional area of the vacuum collection tube,  $\alpha_{\text{stage3}}$  is significantly smaller than stage 2 yet slightly larger than stage 1. Equation 2 provides a summary of relative cross-sectional areas of the current prototype.

$$\alpha_{\text{stage2}} \gg \alpha_{\text{stage3}} > \alpha_{\text{stage1}} \quad (2)$$

These general cross-sectional requirements were used as a guide in designing this first-generation RASTIR source that was made exclusively from commercial parts with one minor modification to the bore size of stage 2. To date, aerodynamic and hydrodynamic injector/ejector devices have been described mathematically using equations of continuity, momentum, energy, and state.<sup>4,5,49,50</sup> However, due to the novelty of these devices in ionization source development, there are not yet reports that account for the addition of an ESI emitter in the exhaust region. Furthermore, these models do not account for the mobility and trajectory of neutral species or how they are entrained within the ESI plume. A more rigorous mathematical description of the RASTIR source will be necessary before optimized designs can be fabricated.

Based on this design, metered nitrogen (primary flow) passes through the 1/8-in. Swagelok fitting (stage 1) and accelerates as it passes through the narrow throat of stage 1. The flow of high-velocity gas from the port connector of stage 1 is directed axially into the 1/16-in. T constituting stage 2 and induces a secondary flow (vacuum) at the terminus of the vacuum collection tube (stage 3).<sup>49</sup> The induced (secondary) flow is in contact with the primary flow and is ejected simultaneously at the exit of the device.<sup>50</sup> From fluid dynamics, there is a limit to the maximum volumetric flow rate that can be achieved in a critical orifice based on its internal diameter and the source of induced vacuum.<sup>51–53</sup> The largest inner diameter of the vacuum collection tube for the current RASTIR

design was 1 mm. The induced vacuum results in pickup of the powder or laser desorbed species, which are entrained as they flow through the device and into the ESI plume (Figure 1A). The “exhaust” component of the RASTIR source (Figure 1A) was positioned ~3 mm from the MS inlet capillary, which was maintained at 37 V. The electrospray plume exits the fused-silica capillary within the exhaust at the exit of stage 2, which allows for interaction of neutrals with the charged solvent droplets resulting in ionized molecules (Figure 1A).

**Applications of RASTIR.** Two sets of experiments were carried out to demonstrate the utility and application of RASTIR. The first experiment was designed to simulate the direct, real-time analysis of an “unknown” powder on a remote solid substrate using a flexible vacuum collection tube. A thin layer of caffeine and acetaminophen powder were deposited onto two glass microscope slides (P/N 12-544-1, Thermo Fisher Scientific, Pittsburgh, PA) shown in an inset picture in Figure 2. A 10-in. flexible section of 1-mm-i.d. PEEK tubing affixed to the RASTIR source (stage 3) was attached as the vacuum collection tube, the electrospray solution was infused at 5  $\mu\text{L}/\text{min}$  at a voltage of 2 kV, and the nitrogen gas was turned on to establish optimized RASTIR conditions. Once the operational conditions of the RASTIR source were established (e.g., establishing ~1-mm distance of the vacuum collection tube from the powder), the LTQ-FT MS was set to continuously collect mass spectra in chromatographic mode while each of the powder samples were collected. Figure 2A shows the resultant total ion chromatograms (TIC) for the two analyte powders collected and ionized by RASTIR over an 8-s time window. The red and green chromatographic traces represents the singly charged caffeine  $[\text{M} + \text{H}]^+$  ( $m/z = 194.08$ ) and acetaminophen  $[\text{M} + \text{H}]^+$  ( $m/z = 151.08$ ) molecules, respectively. The TIC plots show the intermittent nature of the signal that is a potential consequence of the variability in the amount of material removed during the 50-ms LTQ accumulation time, the entrainment efficiency of the particulates in the ESI plume, the particle size, or both. Representative LTQ-FT mass spectra from the TIC (Figure 1A) for caffeine and acetaminophen are shown in Figure 2B and C, respectively. These mass spectra are in agreement with the ionization pathway proposed in FD-ESI, EESI, and similar methods that ionize neutral molecules using some variation of an electrospray plume.<sup>19,20,33–37,54</sup>

A second set of experiments involving the integration of RASTIR with the recently introduced MALDESI source<sup>1,2</sup> was also carried out. MALDESI has the potential to be an ambient ionization source in a multitude of areas including tissue imaging, top-down proteomics, and fundamental ionization mechanism studies. However, a challenge thus far in the implementation of MALDESI (in our experience) has been the isolation of interfering voltages between the MALDI target and the ESI emitter placed in proximity to each other, capture efficiency of the laser-desorbed species by the ESI plume, and elucidation of the fundamental parameters that drive ionization. The RASTIR source provides the potential to overcome these issues thereby allowing MALDESI to emerge as a robust and widely applicable ionization source for the field of mass spectrometry. The MALDESI–RASTIR interface coupled to the LTQ-FT MS inlet is shown in Figure 3A with the dried MALDI spots of BNP-32 and ubiquitin, the vacuum flow direction, and the RASTIR source

(49) Keenan, J. H.; Newman, E. P. *J. Appl. Mech., Trans. ASME* **1942**, *64*, A75–A81.

(50) Fabri, J.; Siestrunk, R. *Advances in Applied Mechanics*; Academic Press: New York, 1958; Vol. V, pp 1–34.

(51) Corn, M.; Bell, W. *Am. Ind. Hyg. Assoc.* **1963**, *24*, 502–504.

(52) Kotrappa, P.; Pimpale, N. S.; Subrahmanyam, P. S. S.; Joshi, P. P. *Ann. Occup. Hyg.* **1977**, *20*, 189–194.

(53) Overcamp, T. J. *Environ. Sci. Technol.* **1985**, *19*, 1134–1136.

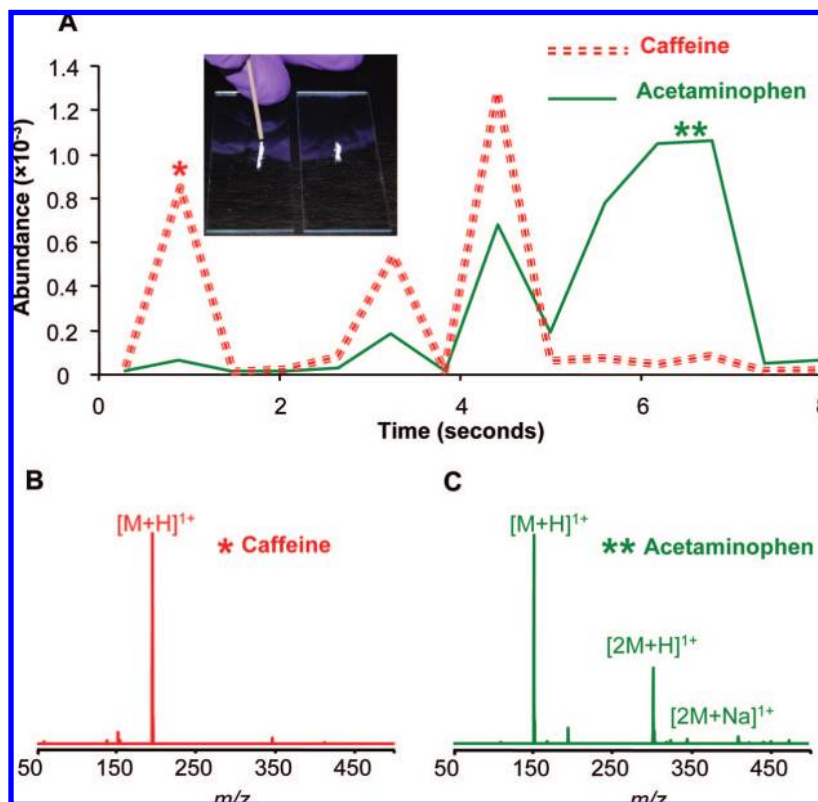


**Figure 2.** A) Total ion chromatogram of caffeine (green) and acetaminophen (red). Insets show the flexible PEEK tubing held over the two powder substrates. (B) Representative positive ion mass spectrum of caffeine (\*) from the TIC. (C) Representative positive ion mass spectrum of acetaminophen (\*\*) from the TIC.

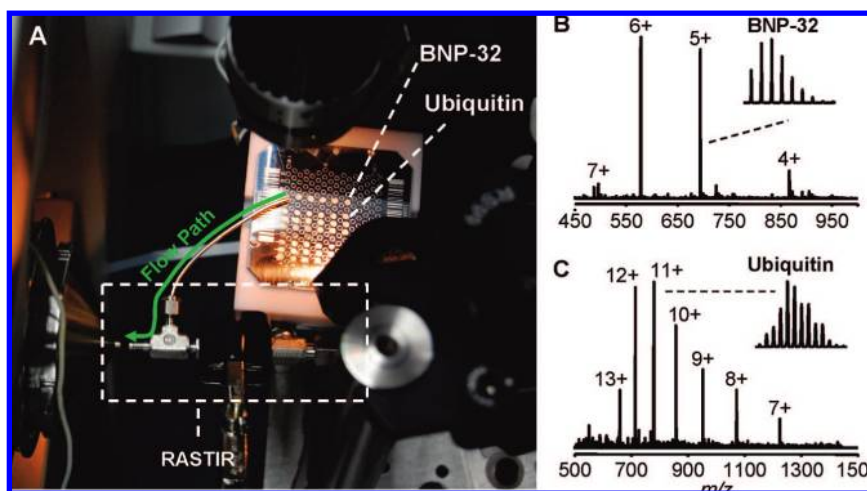


**Figure 3.** (A) Photograph of the MALDESI-RASTIR source interfaced with the LTQ-FT MS. The spotted MALDI target is shown labeled with the BNP-32 and ubiquitin sample spots along with the flow of the vacuum away from the target and toward the mass spectrometer inlet. (B) Representative positive ion mass spectrum of BNP-32 with 4+ through 7+ charge states with a zoom of the 5+ isotopic distribution. (C) Representative positive ion mass spectrum of ubiquitin with showing 7+ through 13+ charge states and a zoom of the 11+ isotopic distribution.

highlighted. Representative LTQ-FT mass spectra of multiply charged BNP-32 ( $\leq 1.3$  pmol) and ubiquitin ( $\leq 2.2$  pmol)<sup>55</sup> generated from the MALDESI-RASTIR source are shown in Figure 3B and C, respectively. The isotopic distributions of the 5+ charge state of BNP-32 and the 11+ charge state of ubiquitin are shown in the Figure 3B and Figure 3C insets, respectively. The charge-state distributions for both BNP-32 and ubiquitin are comparable to standard ESI experiments providing convincing evidence for an ESI mechanism as observed in previous MALDESI,<sup>1,2</sup> FD-ESI,<sup>19,20</sup> and EESI<sup>33–37</sup> reports.

## CONCLUSIONS

The design and implementation of a novel hybrid aerodynamic ionization device (RASTIR) has been described. Two initial “proof of principle” applications of the RASTIR source were demonstrated including the remote capture, transport, and electrospray ionization of powders (caffeine and acetaminophen) and the directed collection, transport, and electrospray ionization of laser desorbed BNP-32 and ubiquitin (MALDESI). Multiple charging was observed in both applications, suggesting ESI as the mechanism for

ionization. The device was constructed for less than \$100 with commercially available components that were slightly modified. Thus, this device could be readily implemented with minimum investment and no foreseeable limitations to use on different MS platforms. Furthermore, RASTIR should be amenable to other ionization sources such as ASAP, APCI, and APPI where remote sampling is warranted. Two inter-related challenges are currently being addressed to better define the analytical figures of merit and improve RASTIR performance. The first is to quantitatively define capture efficiency, limits of detection, and ionization efficiency of RASTIR, and the second is transitioning to a more refined device via mathematical modeling and precision engineering. The goal for these studies will be to develop an analytically robust device that can facilitate potential applications ranging from homeland security and environmental monitoring to tissue imaging and top-down proteomics.

#### ACKNOWLEDGMENT

The authors appreciate enlightening discussions with Professor Jack R. Edwards (NCSU Mechanical and Aerospace Engineering), the photography by Timothy S. Collier, and the use of the NCSU

Analytical Instrumentation Facilities optical microscope. The authors gratefully acknowledge financial support received from the National Institutes of Health (D.C.M., R33 CA105295 and A.M.H., K25 CA128666), the W.M. Keck Foundation, and North Carolina State University.

#### SUPPORTING INFORMATION AVAILABLE

Additional information as noted in text. This material is available free of charge via the Internet at <http://pubs.acs.org>.

Received for review February 11, 2008. Accepted April 23, 2008.

AC800289F

- 
- (54) Dong, J.; Rezenom, Y. H.; Murray, K. K. *Rapid Commun. Mass Spectrom.* **2007**, *21*, 3995–4000.
- (55) The following calculation assumes a homogenous distribution of sample throughout the MALDI spot and that the laser start time = LTQ accumulation start time. Approximately 0.05 mm<sup>2</sup> of material was ablated from a ~4.5-mm<sup>2</sup> MALDI spot size (0.8-μL deposition) that translates to ~1.1% of the MALDI sample removed for a single acquisition. The 1.1% of 155 pmol of BNP-32 (0.8 μL of 144 μM solution) = 1.3 pmol/s and 1.1% of 200 pmol of ubiquitin (0.8 μL of 250 μM solution) = 2.2 pmol/s.